INTERNATIONAL ATOMIC ENERGY AGENCY
UNITED NATIONS EDUCATIONAL, SCIENTIFIC AND CULTURAL ORGANIZATION

INTERNATIONAL CENTRE FOR THEORETICAL PHYSICS
34100 TRIESTE (ITALY) - P.O.B. 586 - MIRAMARE - STRADA COSTIERA 11 - TELEPHONE: 2240-1
CABLE: CENTRATOM - TELEX 460392 - I

SMR/459- 19

SPRING COLLEGE IN CONDENSED MATTER
ON
'PHYSICS OF LOW-DIMENSIONAL SEMICONDUCTOR STRUCTURES'
(23 April - 15 June 1990)

WEAK LOCALIZATION IN THIN FILMS
a time-of-flight experiment with conduction electrons

Gerd BERGMANN
Kernforschungsanlage Jülich GmbH
Institut für Festkorperforschung
Postfach 1913
D-5170 Jülich
Federal Republic of Germany

WEAK LOCALIZATION IN THIN FILMS
a time-of-flight experiment with conduction electrons

Gerd BERGMANN

IFF der KFA, Postfach 1913, 517 Jülich, West-Germany

NORTH-HOLLAND PHYSICS PUBLISHING–AMSTERDAM

PHYSICS REPORTS (Review Section of Physics Letters) 107, No. 1 (1984) 1–58. North-Holland, Amsterdam

WEAK LOCALIZATION IN THIN FILMS
a time-of-flight experiment with conduction electrons

Gerd BERGMANN

IFF der KFA, Postfach 1913, 517 Jülich, West-Germany

Received 15 November 1983

Contents:

Abstract:

The resistance of two-dimensional electron systems such as thin disordered films shows deviations from Boltzmann theory, which are caused by quantum corrections and are called "weak localization". Theoretically weak localization is originated by the Langer–Neal graph in the Kubo formalism. In this review article the physics of weak localization is discussed. It represents an interference experiment with conduction electrons split into pairs of waves interfering in the back-scattering direction. The intensity of the interference (integrated over the time) can be easily measured by the resistance of the film. A magnetic field introduces a magnetic phase shift in the electronic wave function and suppresses the interference after a "flight" time proportional to $1/H$. Therefore the application of a magnetic field allows a time-of-flight experiment with conduction electrons. Spin–orbit scattering rotates the spin of the electrons and yields an observable destructive interference. Magnetic impurities destroy the coherence of the phase. The experimental results as well as the theory is reviewed. The role of the spin–orbit scattering and the magnetic scattering are discussed. The measurements give selected information about the inelastic lifetime of the conduction electrons in disordered metals and raise new questions in solid state physics. Future applications of the method of weak localization are considered and expected.

Single orders for this issue

PHYSICS REPORTS (Review Section of Physics Letters) 107, No. 1 (1984) 1–58.

Copies of this issue may be obtained at the price given below. All orders should be sent directly to the Publisher. Orders must be accompanied by check.

Single issue price Dfl. 35.00, postage included.

1. Introduction

During the past few years a new field in solid state physics has been theoretically and experimentally explored. It deals with the anomalous transport properties of electrons in disordered systems. The phenomenon is generally called weak localization and it is essentially caused by quantum-interference of the conduction electrons on the defects of the systems. Therefore I will also call it alternatively at times "QUIAD" (quantum-interference at defects). This phenomenon had been first considered by Abrahams et al. [1] when they developed a scaling theory for two-dimensional conductors. In their work weak localization was only an asymptotic case of a more general theory. But soon it became a field on its own with growing importance. During the mean-time extensive theoretical work [2–84] as well as experimental investigations on metals [85–128] (thin films) and [129–134] (one- and three-dimensional metals) and MOS inversion layers and other semiconductors [135–153] have followed. In particular the resistance anomaly at low temperature and the magneto-resistance have been intensively studied.

Weak localization exists in one, two and three dimensions as well but for an experimental investigation the two-dimensional case is the most favourable one. Here the correction to the resistance is of the order of 10^{-2} to 10^{-3} and can be easily measured with an accuracy of 1%. One can in particular investigate the QUIAD in two dimensions in a magnetic field perpendicular to the film (which is not possible in one dimension). We will see that the response to a magnetic field is a powerful method to determine characteristic times of the electron system. The physical reason is that weak localization corresponds to a time-of-flight experiment with conduction electrons. Therefore most of the experimental work on metals is done in thin films. Another two-dimensional electronic system has been experimentally investigated as well – electron inversion layers. Since many properties of the electronic system in inversion layers are quite different from the metal I leave the discussion of inversion layers to an expert in that field and concentrate here on two-dimensional thin films.

Since one can prepare thin films of every metal and most alloys QUIAD allows to study many materials with quite different properties such as simple metals, transition metals, superconductors, nearly magnetic metals, etc. The experimental investigation is only at the beginning but in the past it has been shown that weak localization exists, can be well described by the theory and allows to measure characteristic times of the electron system such as inelastic lifetime, spin–orbit scattering time and magnetic scattering time. However, the use of this new method has just been started, there is no systematic investigation of the large variety of materials yet.

The aim of this article is to introduce the reader into the physics of QUIAD. Section 2 concentrates on the physics of weak localization (it is essentially an extended version of a lecture the author used to deliver on weak localization). Here the complicated Kubo graph of the theory is translated into a simple physical picture. It is shown that weak localization is a rather sophisticated but transparent interference experiment.

Section 3 deals with the theory of weak localization, repeats shortly the Kubo formalism and evaluates the Langer–Neal graph in some detail. Although being a theoretical section it is written for the interested experimentalist. The plan for this section was stimulated from the difficulties which the author had with several theoretical papers in this field because they were so condensed. In particular it was often rather difficult to modify the theoretical calculations which is for example necessary if one wants to generalize a strictly two-dimensional calculation to a film of finite thickness. The large amount of non-economic work which I had to invest into some of the theoretical papers to read between the lines lead me to the conclusion that an extended section on the theory might be of some use for other interested experimentalists. Theoreticians are referred to the review articles by Fukuyama [76] and Altshuler and Aronov [154].

Since the formulae which the theory derives are not really transparent section 4 gives a graphic evaluation of these formulae to show the structure of the theory.

Section 5 describes and collects the experimental results on magneto-resistance, temperature dependence, electric field dependence, magnetic scattering, etc.

One of the most interesting experimental results of QUIAD is the measurement of the inelastic lifetime. The theoretical aspects as well as the experimental results are discussed in section 6.

Since the Coulomb interaction in disordered two-dimensional electron systems yields a similar resistance anomaly with temperature as weak localization does the properties of electron–electron interaction are briefly sketched in section 7.

Finally we discuss some of the future applications of weak localization in solid state physics in section 8.

2. Physical interpretation of weak localization

Thin disordered metal films show resistance anomalies which were theoretically not understood until five years ago. Fig. 2.1 shows the magneto-resistance of a thin Cu-film with a thickness of 80 Å and a high degree of disorder. Its electronic mean free path is only of the order of 10 Å. The resistance (per square) changes in a magnetic field perpendicular to the film and the magneto-resistance is strongly temperature dependent. According to the classical theory the resistance should be completely field independent because the product $\omega_c\tau_0$ is (even in a field of 7 T) only of the order of 10^{-4} and the magneto-resistance is proportional to the square of $\omega_c\tau_0$. ($\omega_c = He/m$ = cyclotron frequency and τ_0 = elastic scattering time.) The unexpected magneto-resistance is a manifestation of the new

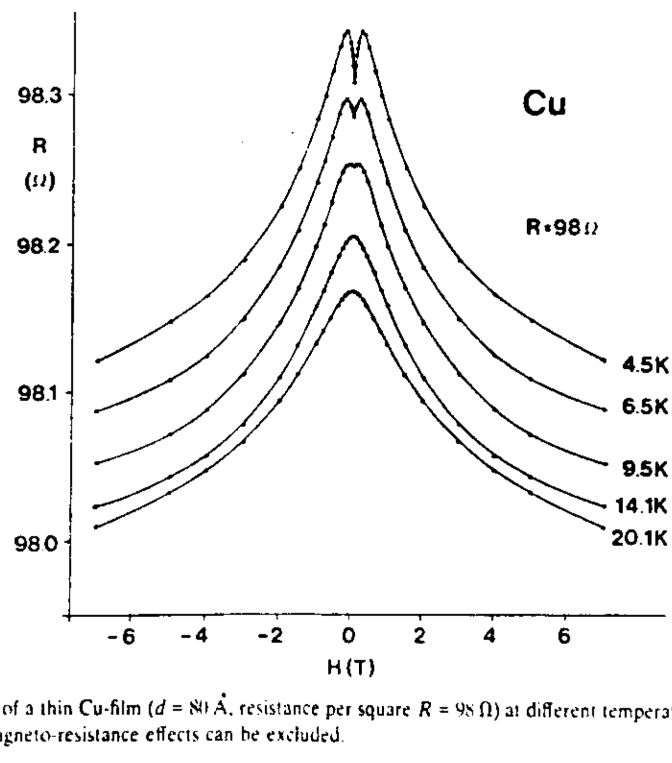

Fig. 2.1. The magneto-resistance of a thin Cu-film (d = 80 Å, resistance per square R = 98 Ω) at different temperatures. The mean free path is of the order of 10 Å so that classical magneto-resistance effects can be excluded.

phenomenon which is generally called weak localization. In this section we want to point out that weak localization corresponds to an interference experiment with conduction electrons which are scattered at impurities [155]. The application of a magnetic field influences this interference and introduces a time scale into the system. Finally we will recognize that the magnetic field allows to observe the fate of the conduction electrons as a function of time.

At low temperature one has to distinguish between two different lifetimes of the conduction electrons, the elastic lifetime τ_0 and the inelastic lifetime τ_i. Here τ_0 is the lifetime of the electron in an eigenstate of momentum, whereas τ_i is the lifetime in an eigenstate of energy. At 4 K, the latter can exceed the former by several orders of magnitude. As a consequence, a conduction electron in state k can be scattered by impurities without loosing its phase coherence. Due to the statistical distribution of the impurities, the multiple scattered waves form a chaotic pattern. The usual Boltzmann theory neglects interferences between the scattered partial waves and assumes that the momentum of the electron wave disappears exponentially after the time τ_0 (or τ_{tr} = transport mean free path. In the following consideration we assume s scattering so that τ_0 and τ_{tr} are equal). This assumption yields for free electrons the simple Drude formula for the conductivity

$$\sigma = \frac{ne^2}{m}\tau_0 . \tag{2.1}$$

The neglect of the interference is, however, not quite correct. There is a coherent superposition of the scattered electron wave which results in back-scattering of the electron wave and lasts as long as its coherence is not destroyed. This causes a correction to the conductance which is generally calculated in the Kubo formalism by evaluating "Kubo graphs". The most important correction has already been discussed by Langer and Neal [156] in 1966 and is shown in fig. 2.2a. This Langer–Neal graph has been evaluated by Abrahams et al. [1] for two-dimensional disordered systems of finite size and they concluded that a two-dimensional conductor with a finite concentration of defects becomes an insulator at $T = 0$ K. Anderson et al. [2] and Gorkov et al. [4] showed that at low but finite temperature the conductance has a correction

$$\Delta L = -\Delta R/R^2 = L_{00}\log(\tau_i/\tau_0)\,; \qquad L_{00} = e^2/(2\pi^2\hbar)\,. \tag{2.2}$$

This correction is temperature dependent because the inelastic lifetime depends on the temperature (for example $1/\tau_i \propto T^p$). In the following we will translate the Langer–Neal graph into a transparent physical picture and show that it corresponds to an interference experiment.

2.1. *The echo of a scattered conduction electron*

We consider at the time $t = 0$ an electron of momentum $\boldsymbol{k}$ which has the wave function $\exp[i\boldsymbol{kr}]$. The electron in state $\boldsymbol{k}$ is scattered after the time τ_0 into a state $\boldsymbol{k}'_1$, after $2\tau_0$ into the state $\boldsymbol{k}'_2$, etc. There is a finite probability that the electron will be scattered into the vicinity of the state $-\boldsymbol{k}$; for example after n scattering events. This scattering sequence (with the final state $-\boldsymbol{k}$)

$$\boldsymbol{k} \to \boldsymbol{k}'_1 \to \boldsymbol{k}'_2 \to \cdots \to \boldsymbol{k}'_{n-1} \to \boldsymbol{k}'_n = -\boldsymbol{k}$$

is drawn in fig. 2.2b in k-space. The momentum transfers are $\boldsymbol{g}_1, \boldsymbol{g}_2, \ldots, \boldsymbol{g}_n$. There is an equal

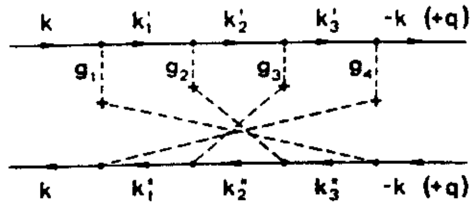

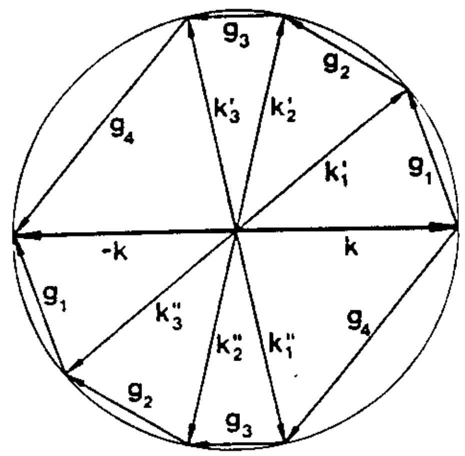

Fig. 2.2. (a) The fan diagram, introduced by Langer and Neal, which allows calculations of quantum corrections to the resistance within the Kubo formalism. (b) The physical interpretation of the fan diagram in (a). The electron in the eigenstate of momentum k is scattered via two complementary series of intermediate scattering states $k \to k'_1 \to k'_2 \to \cdots \to k'_{n-1} \to k'_n = -k$ and $k \to k''_1 \to k''_2 \to \cdots \to k''_{n-1} \to k''_n = -k$ into the state $-k$. The change of momentum is $g_1, g_2, \ldots, g_{n-1}, g_n$ for the first series and $g_n, g_{n-1}, \ldots, g_2, g_1$ for the second. The amplitudes in the final state $-k$ are identical, $A' = A'' = A$ and interfere constructively, yielding an echo in back-scattering direction which decays as $1/t$ in two dimensions. Only for times longer than the inelastic lifetime τ_i the coherence is lost and the echo disappears.

probability for the electron k to be scattered in n steps from the state k into $-k$ via the sequence

$$k \to k''_1 \to k''_2 \to \cdots \to k''_{n-1} \to k''_n = -k$$

where the momentum transfers are $g_n, g_{n-1}, \ldots, g_1$. This complementary scattering series has the same changes of momentum in opposite sequence. If the final state is $-k$, then the intermediate states for both scattering processes lie symmetric to the origin. The important point is that the amplitude in the final state $-k$ is the same for both scattering sequences. This is caused essentially by the proportionality of the final amplitude to the product of the matrix elements i.e. $\Pi\, V(g_i)$ – where $V(g_i)$ is the Fourier component of the scattering potential – and this product is the same for both sequences. Secondly the transition probability is identical because of the symmetry of the two complementary processes. In addition the energy of the corresponding intermediate states is (by pairs) the same so that the time-dependent phase changes ($Et/\hbar$) are identical.

Since the final amplitudes A' and A'' are phase coherent and equal, $A' = A'' = A$, the total intensity is $|A' + A''|^2 = |A'|^2 + |A''|^2 + A'^*A'' + A'A''^* = 4|A|^2$. If the two amplitudes were not coherent then the total scattering intensity of the two complementary sequences would only be $2|A|^2$. This means that the scattering intensity into the state $-k$ is by $2|A|^2$ larger than in the case of incoherent scattering. This additional scattering intensity exists only in the back-scattering direction. For other states at the Fermi surface, sufficiently far away from $-k$, there is only an incoherent superposition of every two sequences (with momentum transfer in the opposite sequence) and therefore as an average the scattering intensity per sequence with n scattering processes is only $|A|^2$.

The fan diagram in fig. 2.2a gives just the product A'^*A'', i.e. the interference intensity. It consists of two parts, the upper electron propagator and the lower hole propagator. The upper one yields the amplitude of the electron k which is scattered into the state $-k$ via the scattering sequence ('). If we invert the direction of the arrows for the lower propagator then it yields the amplitude of the electron k which is scattered into the state $-k$ via the scattering sequence ("). The reversed direction of the arrows (i.e. that it is a hole propagator) yields the complex conjugate of the amplitude.

At high temperature the scattering processes are partially inelastic. As a consequence the amplitudes A' and A'' loose their phase coherence (after the time τ_i) and the intensity of the back-scattered wave is only $2|A|^2$, i.e. the coherent back-scattering disappears after the time τ_i. In fig. 2.3 the momentum of the electron k is plotted as a function of time. The original momentum decays within the elastic lifetime τ_0. At later times a momentum in the opposite direction is formed; this decreases inversely proportional to the time (as we shall see below). One obtains an echo of the original state k in opposite direction which vanishes only when the two processes loose their coherence. Obviously the integrated momentum of the electron k decreases with increasing τ_i. In the following we treat this scattering semi-quantitatively.

After the elastic lifetime τ_0 the electron k is scattered into a shell at the Fermi surface which is assumed to contain Z intermediate states. The amplitude in the intermediate state k_1' is $Z^{-1/2}\,e^{i\delta_1}$ where $e^{i\delta_1}$ is essentially given by $V(g_1)/|V(g_1)|$. The intensity in the next intermediate state k_2' at the time $2\tau_0$ is Z^{-2}. After n scattering processes the intensity in the final state $-k$ is Z^{-n} and the amplitude $Z^{-n/2}\,e^{i\Sigma\delta_\nu}$. The second scattering series yields the same amplitude. The cross product or interference term is $A'^*A''+A'A''^*=2Z^{-n}$. Now we have to sum over all possible intermediate states. This yields the factor $1/2\,Z^{n-1}$. (1/2 occurs because the two complementary series appear twice in the sum.) Therefore the coherent additional back-scattering intensity is Z^{-1}. It is independent of the number of intermediate scattering states n and equal to the scattering intensity from k into k_1'. This intensity is, of course, completely calculated in evaluating the diagram with the appropriate rules. However, one can easily estimate this intensity in a rather direct and less formal manner.

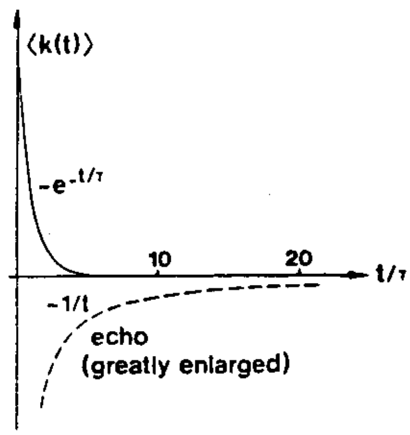

Fig. 2.3. The contribution of the electron state k to the momentum as function of time. The original state and its momentum decay exponentially within the time τ_0 (s scattering assumed). But an echo with the momentum $-k$ is formed which depends on time as $1/t$. This echo reduces the contribution of the electron to the current and yields a correction to the resistance which is proportional to $\log(\tau_i/\tau_0)$.

For the calculation of Z in two dimensions we consider the scattering from the state k into the state k'_1. This state is an intermediate state for the scattering sequence which does not have to conserve the energy (sometimes called virtual scattering process). Since the elastic lifetime is τ_0 the intermediate state can lie within $\pi\hbar/\tau_0$ of the Fermi energy. This corresponds to a smearing of the Fermi sphere by π/l (l = mean free path of the conduction electrons). Therefore the available area in k-space is $2\pi k_F * \pi/l = 2\pi^2 k_F/l$ and Z is obtained by multiplying by the density of state in k-space, i.e. $(2\pi)^{-2}$.

The coherent back-scattering is not restricted to the exact state $-k$; one has a small spot around the state $-k$ in momentum space which contributes. We calculate the coherent back-scattering intensity into the state $-k + q$ which is reached after n scattering processes with the transfer of momentum g_i where $\Sigma g_i = -2k_F + q$. The sum of the momenta of the initial and final state is $+q$. The same applies for each pair of scattering states in fig. 2.2b which lie opposite to the centre, i.e. $q = k'_1 + k''_{n-1} = k'_2 + k''_{n-2} = \dots$ The corresponding intermediate states differ not only in momentum but also in energy (which must not be conserved). The energy difference is $\hbar q * v_F$ and since the phase rotates with $Et/\hbar$ one obtains during the time τ_0 a phase difference between the two complementary waves which is $q * v_F\tau_0$. The important fact is that the different intermediate states have independent directions of momentum. Therefore the phase differences are independent in sign and value. This means that only the square of the phase shifts adds. Therefore after the n scattering processes one obtains phase differences between the complementary waves whose width is

$$[\Delta\varphi]^2 = n\,\overline{(q * v_F\tau_0)^2} = n\,\tfrac{1}{2}(v_F q\tau_0)^2 = nDq^2\tau_0\,. \tag{2.3}$$

In two dimensions the average over $(v_F * q)^2$ is $(v_F q)^2/2$ (and in three dimensions $(v_F q)^2/3$ but the diffusion constant absorbs the factor of dimension). The neighbouring states of $-k$ contribute less to the coherent back-scattering because they loose the phase coherence with increasing n and q. Their contribution is proportional to $\exp[-Dq^2 t]$ since $t = n\tau_0$. The area of the spot for the coherent back-scattering is obtained by integration over q. In two dimensions this yields $\pi/(Dt)$. This corresponds to about $\pi(Dn\tau_0)^{-1}/(2\pi)^2$ states, i.e. their number shrinks with time. Therefore the portion of coherent back-scattering is given by

$$I_{\rm coh} = [\pi/(Dt)]/[2\pi^2 k_F/l] = \tau_0/(\pi k_F l t) = \hbar/(2\pi E_F t)\,. \tag{2.4}$$

In the presence of an external electrical field the conduction electrons contribute to the current. However, the echo, i.e., the coherent back-scattering reduces the current and therefore the conductance. A pulse of an electrical field generates a short current (for the time τ_0) in the direction of the electric field and then a reversed current which decays as $1/t$. The dc conductance is obtained by integrating the momentum over time. For the normal contribution this yields $k\tau_0$ and for the echo $[k\tau_0/(\pi k_F l)]\ln(\tau_i/\tau_0)$. Therefore the electron in the state k contributes to momentum

$$k\tau_0\{1 - [1/(\pi k_F l)]\ln(\tau_i/\tau_0)\}\,. \tag{2.5}$$

The contribution of the electron k to the current is reduced by the factor in the brackets and the conductance is decreased by the same factor,

$$L = (ne^2\tau_0/m) * \{1 - [1/(\pi k_F l)]\ln(\tau_i/\tau_0)\}$$
$$= (ne^2\tau_0/m) - [e^2/(2\pi^2\hbar)] * \ln(\tau_i/\tau_0) \tag{2.6}$$

with $n = 2\pi k_F^2/(2\pi)^2$. This correction to the conductance was introduced by Anderson et al. [2] and Gorkov et al. [4].

The important consequence of the above consideration is that the conduction electrons perform a typical interference experiment. The (incoming) wave k is split into two complementary waves k_i' and k_i''. The two waves propagate individually, experience changes in phase, spin orientation, etc. and are finally unified in the state $-k$ where they interfere. The intensity of the interference is simply measured by the resistance. In the situation which has been discussed above the interference is constructive in the time interval from τ_0 to τ_i. It is only slightly more complicated than a usual interference experiment because one has a larger number of pairs of complementary waves.

Shortly after the development of the theory several experimental groups investigated the resistance of thin disordered films (and MOS inversion layers) as a function of temperature and found indeed an increase of the resistance with the logarithm of the (decreasing) temperature. Figs. 2.4a–c show results by Dolan and Osheroff [85] on thin AuPd-films, and Van den dries et al. [87] and Kobayashi et al. [86] on thin Cu-films. These experimental results appeared to be an experimental proof of the theory of weak localization. However, a few months later Altshuler et al. [157] showed that there is another effect in two-dimensional disordered systems which causes essentially the same resistance anomaly with temperature. They showed that in disordered electron systems the Coulomb interaction is modified. The electron–electron interaction is dynamically not perfectly screened but long ranged. This has an important impact on the density of states as well as on the resistance of disordered two-dimensional electron systems. We shall return to the effect of the Coulomb interaction in section 7. As a consequence of this alternative mechanism one had to look for a more characteristic experimental investigation of weak localization. The application of a magnetic field provided such a possibility.

2.2. *Time-of-flight experiment in a magnetic field*

One of the interesting possibilities for an interference experiment is to shift the relative phase of the two interfering waves. For charged particles this can be easily done by an external magnetic field.

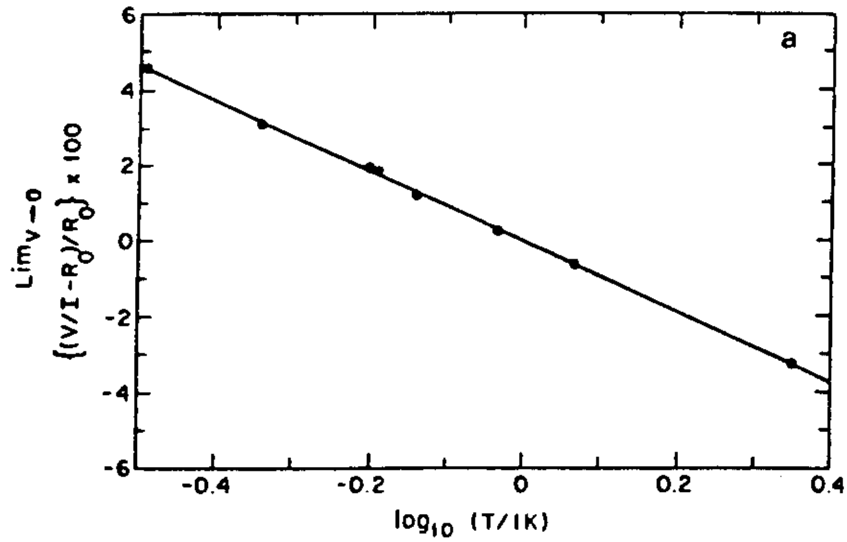

Fig. 2.4(a)

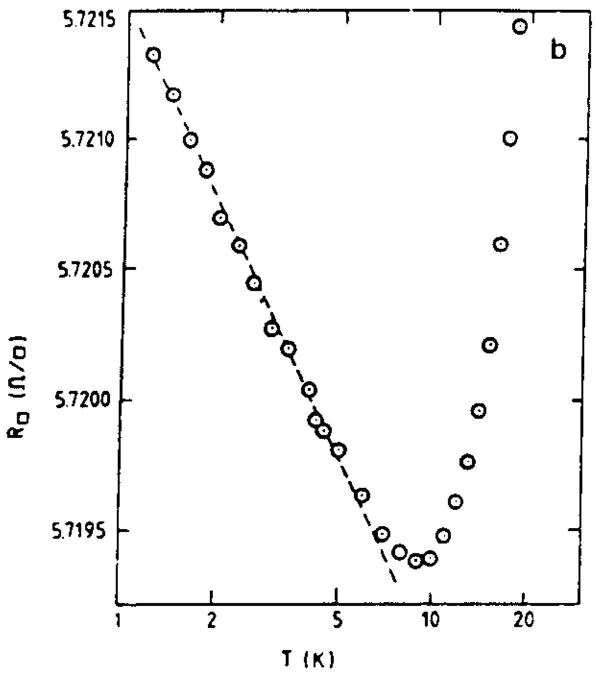

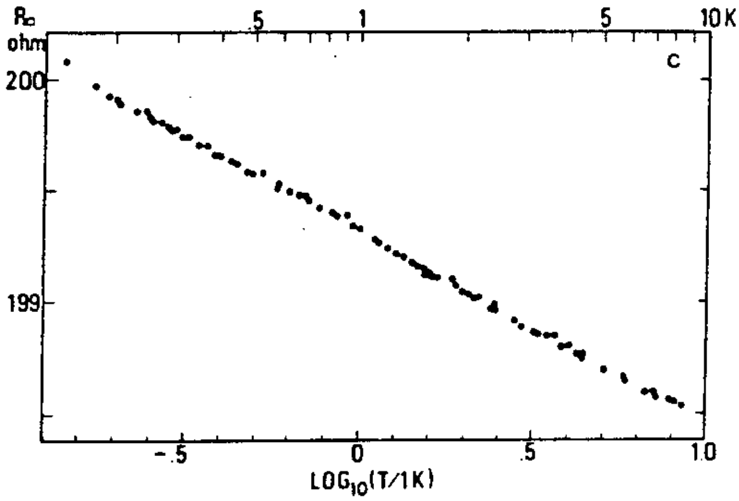

Fig. 2.4. The resistance of thin disordered films as function of the logarithm of the temperature. (a) a AuPd-film by Dolan and Osheroff [85], (b) a Cu-film by Van den dries et al. [87] and (c) coupled fine Cu-particles by Kobayashi et al. [86].

Before we treat the effect of a magnetic field in some detail we consider the motion of the conduction electron in real space. Since the conduction electron has a very short mean free path it diffuses in the two-dimensional conductor from impurity to impurity. Consider an electron at the origin at $t = 0$. The classical diffusion equation in two dimensions yields for the probability (density) of finding the electron at the time t at the position r

$$p(r, t) = [1/(4\pi Dt)] * \exp[-r^2/(4Dt)] . \tag{2.7}$$

The chance to return to the origin is given by $1/(4\pi Dt)$. In fig. 2.5 a possible path is drawn for the diffusion of an electron which returns to the origin. For classical diffusion one has an identical probability for the electron to propagate on the same path in the opposite direction. The two probabilities add up and contribute to the total probability of $1/(4\pi Dt)$. Since the electron has wave-like character in reality one has to consider two partial waves of the electron which propagate in opposite directions on the indicated path. Returned to the origin, however, their amplitudes add (instead of their intensities). It is the same physical mechanism which has been discussed in momentum space before. This picture has been used by Altshuler et al. [26] in studying the electric field effect on QUIAD. The amplitudes A' and A'' are equal because their partial waves propagated on the same path in opposite directions and as long as the system shows time reversal the two partial waves arrive at the origin in phase and with the same amplitude. Therefore the intensity or probability is twice as large as in the classical diffusion problem i.e. $1/(2\pi Dt)$. For the diffusion to any other point except the vicinity of the origin the different partial waves are generally incoherent and only their intensities add. (There is only a small reduction to compensate the increased intensity at the origin.) In fig. 2.6 the classical and the quantum diffusion probabilities are plotted qualitatively. The (dashed) peak in quantum diffusion at the origin describes a tendency to remain at or return to the origin. Since it is thought of as a precursor of localization this quantum diffusion has been called weak localization. (A localized electron would

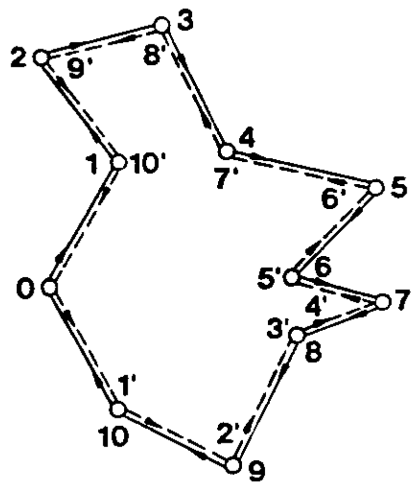

Fig. 2.5. Diffusion path of the conduction electron in the disordered system. The electron propagates in both directions (full and dashed lines). In the case of quantum diffusion the probability to return to the origin is twice as great as in classical diffusion since the amplitudes add coherently.

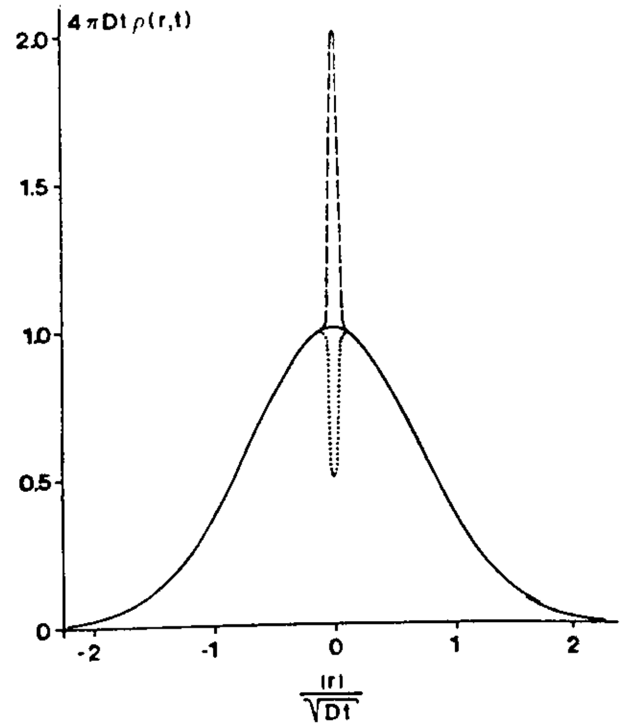

Fig. 2.6. The probability distribution of a diffusing electron which starts at $r = 0$ at the time $t = 0$. In quantum diffusion (dashed peak) the probability to return to the origin is twice as great as in classical diffusion (full curve). Large spin–orbit scattering reduces the probability by a factor of two (dotted peak) and yields a weak anti-localization.

remain close to the origin.) This name is, however, questionable because in the presence of large spin–orbit scattering – as we discuss below – the quantum diffusion yields a reduced probability (dotted peak) to return to the origin, an effect one might call weak anti-localization [46].

In a magnetic field, however, the phase coherence of the two partial waves is weakened or destroyed. When the two partial waves surround an area F containing the magnetic flux ϕ, then the relative change of the two phases is $(2e/\hbar)\phi$. The factor of 2 arises because the two partial waves surround the area twice. (This is sometimes interpreted as if a particle with twice the electron charge surrounds the area in analogy to the double charge $2e$ in superconductivity.)

Since the diffusion is statistical for a given diffusion time t a whole range of enclosed areas for the different diffusion paths exists. Altshuler et al. [19] suggested performing such an "interference experiment" with a cylindrical film in a magnetic field parallel to the cylinder axis. Then the magnetic phase shift between the complementary waves is always a multiple of $2e\phi/\hbar$ (ϕ = flux in the area of the cylinder). Sharvin and Sharvin [92, 102] showed in a beautiful experiment that then the resistance oscillates with a flux period of $\phi = h/(2e)$. Fig. 2.7a shows the geometry of a thin cylindrical film and fig. 2.7b the oscillation of the resistance for a thin cylindrical Mg-film [92].

However, for a thin film in a perpendicular magnetic field the pairs of partial waves enclose areas between $-2Dt$ and $2Dt$. When the largest phase shift exceeds 1, the interference is both constructive and destructive as well and the average cancels. This happens roughly after the time $t_H = \hbar/(4eDH)$. This means essentially that the conductance correction in the field H i.e. $\Delta L(H)$ yields the coherent back-scattering intensity by integrating from τ_0 to t_H

$$\Delta L(H) \propto \int_{\tau_0}^{t_H} I_{\mathrm{coh}}\, \mathrm{d}t \propto -L_{00} \log(t_H/\tau_0)\,. \tag{2.8}$$

It is important to mention that only the amplitudes of the "scattered" waves interfere. There is no interference between the original wave function and its scattered component considered in this theory and at these finite temperatures the coherence length, i.e. the length over which a wave packet can be defined at finite temperature and which is of the order of $\hbar v_F/(k_B T)$ is much smaller than the inelastic mean free path $v_F\tau_i$. (Otherwise one is no longer in the region of QUIAD.)

The quantitative calculation yields a simple result. The application of a magnetic field causes a destructive interference in the final state $-\boldsymbol{k}$. But in the vicinity of $-\boldsymbol{k}$ for the states $-\boldsymbol{k}+\boldsymbol{q}$ the interference is constructive if $\boldsymbol{q}$ lies on Landau-like circles with $(\hbar q)^2/(4m) = \hbar\omega_c(n+\frac{1}{2})$ where ω_c is the cyclotron frequency. The allowed states as a function of $\boldsymbol{q}$ are shown in fig. 2.8. (The electron states on the "Landau circles" are not free electron states in a magnetic field because they are centred around $-\boldsymbol{k}$. Only formally they correspond to hypothetical particles with twice the electron mass.) Since, on the other hand, the width of the coherently back-scattered spot shrinks with time as $(Dt)^{-1/2}$ the coherent back-scattering dies out when the spot lies completely inside the first Landau circle with the radius $(2eH/\hbar)^{1/2}$. This occurs for fields of the order of $H = \hbar(4eDt)$.

This means that the magnetic field allows a time-of-flight experiment. If a magnetic field H is applied the contribution of coherent back-scattering is integrated in the time interval between τ_0 and $t_H = \hbar/(4eDH)$. If one reduces the field from the value H' to the value H'' and measures the change of resistance this yields the contribution of the coherent back-scattering in the time interval $t_{H'}$ and $t_{H''}$. In a very strong field the coherent interference is suppressed. A reduction of the field integrates the coherent back-scattering and increases the resistance. If t_H exceeds the inelastic lifetime of the

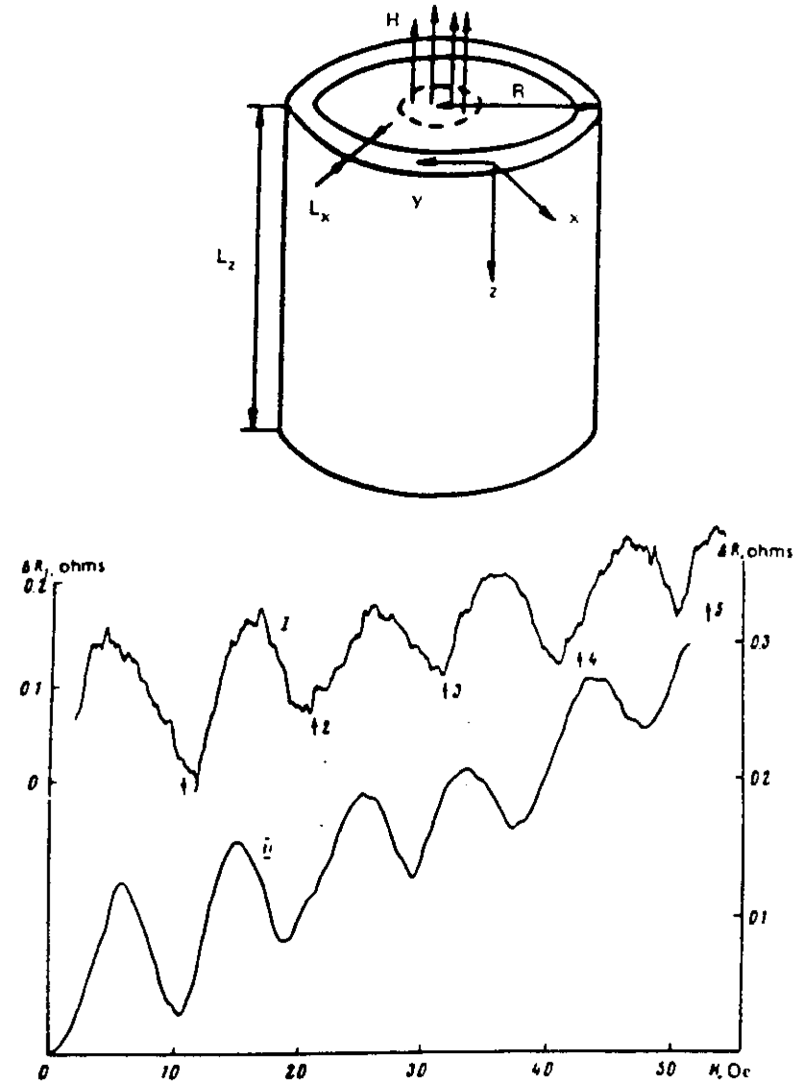

Fig. 2.7. Aranov–Bohm effect in a disordered hollow cylinder in a magnetic field parallel to the cylinder axis as suggested by Altshuler and Aronov [19]. (a) the geometry, (b) the resistance oscillation as a function of the applied magnetic field measured by Sharvin and Sharvin [92] on a cylindrical Mg-film.

conducting electrons, i.e. $H < H_i = \hbar/(4eD\tau_i)$ then the coherence is lost anyway and the magneto-resistance disappears. Since the magnetic field introduces a time t_H into the electron system all characteristic times τ_n of the electrons can be expressed in terms of magnetic fields H_n,

$$\tau_n \Leftrightarrow H_n \tag{2.9}$$

where $\tau_n H_n = \hbar/(4eD)$. In a thin film this is given by $\hbar e\rho N/4$ which is of the order of 10^{-12} to 10^{-13} Ts (ρ = resistivity of the film and N = density of electron states for both spin directions). A magnetic field of 1 T corresponds to about 0.1–1 ps, i.e. the magneto-resistance measurement allows picosecond

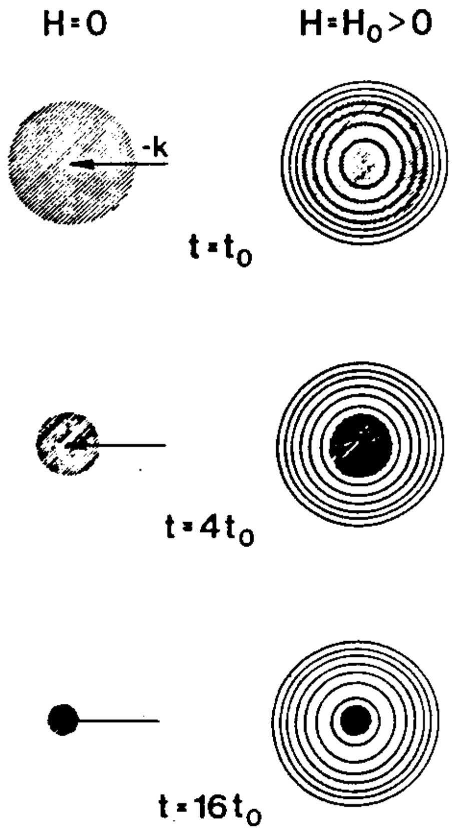

Fig. 2.8. The back-scattering spot (close to the state $-k$) without magnetic field (left side) and in a finite magnetic field H. The spot has a finite area $\pi(Dt)$ which shrinks with time. In a magnetic field the coherence condition is modified and only k states which lie on "Landau"-like circles allow coherent back-scattering. For long time t the two interference conditions exclude each other because the spot is inside of all "Landau" circles and the coherent back-scattering dies at a time $t_H = \hbar/(4eDH)$. The resistance integrates the coherent back-scattering intensity in the time interval from τ_0 to t_H.

spectroscopy with the conduction electrons. The exact formulae for the magneto-conductance are derived in section 3.

The motion of the conduction electron in real space gives a simple criterion for the conditions under which a thin film is two-dimensional [27, 53, 91]. The important requirement for the quantum interference is that the electron wave function is coherent. Therefore a system is two-dimensional with respect to QUIAD when its coherence volume has a two-dimensional shape. Without a magnetic field the electron diffuses during its inelastic lifetime over a distance of $(D\tau_i)^{1/2}$. If the thickness of the film is much less than this "Thouless length" then the region of coherence is two-dimensional. For films thinner than 100 Å thickness and at temperatures below 20 K this requirement is generally very well fulfilled. However, in strong magnetic fields the distance of coherent diffusion $(Dt_H)^{1/2}$ is much less and therefore one easily moves into the three-dimensional range. Therefore one expects deviations from the two-dimensional formula in high magnetic fields (one has to include the sheets in k-space for $k_z = \nu * \pi/d$; d = film thickness, see sections 3 and 5).

Before we turn to the evaluation of the experimental magneto-resistance curves we have to discuss the influence of the spin–orbit scattering.

2.3. Spin–orbit scattering

One of the most interesting questions in QUIAD is the influence of spin–orbit scattering [7, 8, 24]. Hikami et al. [7] predicted in the presence of strong spin–orbit scattering a logarithmic decrease of the resistance with decreasing temperature. As a consequence the magneto-resistance should change sign as well. This prediction is contrary to the picture of localization and was one of the most exciting questions at LT XVI. The prediction by Hikami et al. could be experimentally confirmed by the author [96]. For this purpose a thin Mg-film has been prepared in an ultra high vacuum. Mg is a light metal and has a very small spin–orbit coupling. The upper part of fig. 2.9 shows the magneto-resistance of the pure Mg-film at different temperatures. After the measurement the Mg-film has been covered with 1/100 layer of the strong spin–orbit coupler Au. This causes a significant change of the magneto-resistance as is shown in the lower part of fig. 2.9. At low temperature the magneto-resistance changes sign and shows a substructure which reflects the strength of the spin–orbit scattering. In fig. 2.10 the magneto-resistance of another Mg-film at 4.5 K is plotted for increasing coverage with Au. The points represent the experimental results, whereas the full curves are calculated with the theory of Hikami et al. The adjustable parameter is the spin–orbit scattering time which decreases with increasing Au coverage (this experiment also yields the spin–orbit scattering of the pure Mg-film). Obviously weak localization provides a new and very sensitive method to measure the spin–orbit scattering directly, i.e. with a substructure and not only by a broadening of a resonance.

Now we can turn to the evaluation of the magneto-resistance curves of pure Mg. In fig. 2.11 the magneto-resistance of a Mg-film is plotted as a function of the applied magnetic field [97]. The units of the field are shown on the right side of the curves. The Mg is quench-condensed at helium temperature.

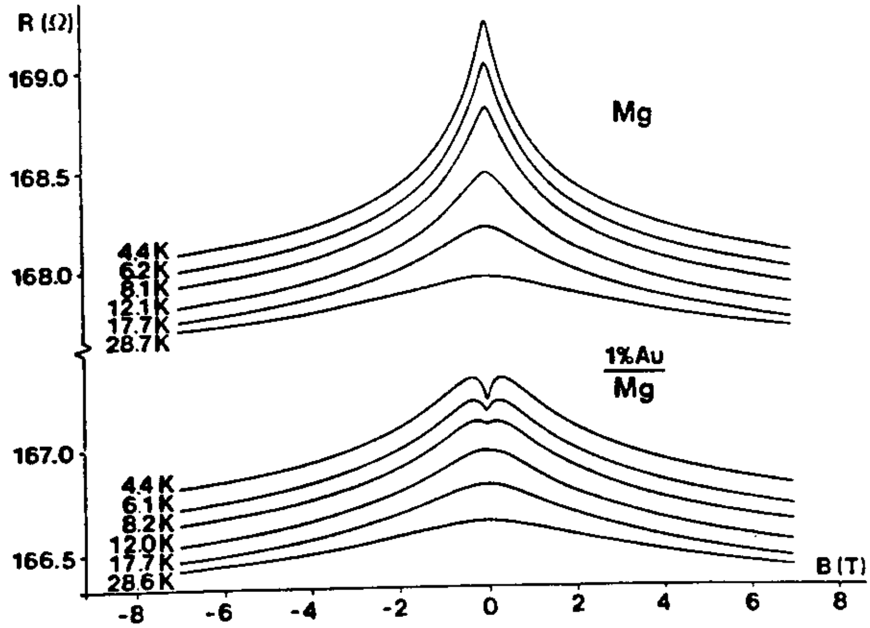

Fig. 2.9. The magneto-resistance curves of a thin Mg-film (upper set of curves). After a superposition with 1/100 atomic layer of Au the magneto-resistance changes drastically. The Au introduces a rather pronounced spin–orbit scattering which rotates the spins of the complementary scattered waves. This changes the interference from constructive to destructive.

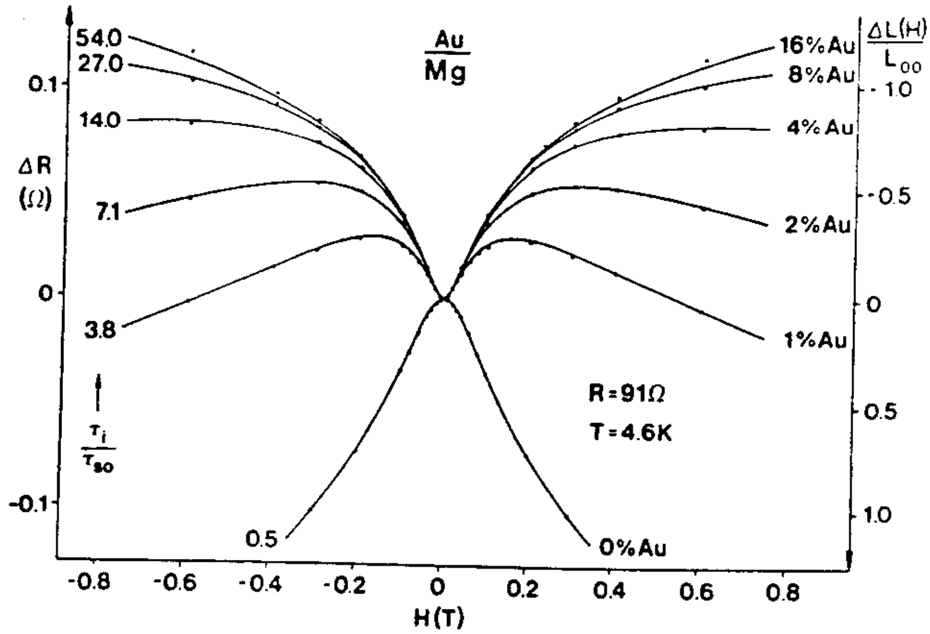

Fig. 2.10. The magneto-resistance of a thin Mg-film at 4.5 K for different coverages with Au. The Au thickness is given in % of an atomic layer on the right side of the curves. The superposition with Au increases the spin–orbit scattering. The points are measured. The full curves are obtained with the theory by Hikami et al. The ratio τ_i/τ_{so} on the left side gives the strength of the adjusted spin–orbit scattering. It is essentially proportional to the Au-thickness.

because the quenched condensation yields homogeneous films with high resistances. The points are measured. The spin–orbit scattering of the pure Mg is determined as discussed above. The different experimental curves for different temperatures are theoretically distinguished by their different H_i (i.e. the inelastic lifetime). This is the only adjustable parameter for a comparison with theory (after H_{so} is determined). The ordinate is completely fixed by the theory in the universal units of L_{00} (right scale). The full curves give the theoretical results with the best fit of H_i which is essentially a measurement of H_i. The agreement between the experimental points and the theory is very good. The experimental result proves the destructive influence of a magnetic field on QUIAD. It measures the area in which the coherent electronic state exists as a function of temperature and allows the quantitative determination of the coherent scattering time τ_i. The temperature dependence is given by a T^{-2} law for Mg as is shown in fig. 2.12.

For other metal films where the nuclear charge is higher than in Mg one finds even in the pure case the substructure caused by spin–orbit scattering. In fig. 2.13 the magneto-resistance curves for a thin quench condensed Cu-film are shown. Again the points represent the experimental results whereas the full curves show the theory. At low temperatures the inelastic lifetime is long and therefore the effect of the spin–orbit scattering dominates in small fields. At high temperatures the inelastic lifetime becomes smaller than the spin–orbit scattering time and the magneto-resistance becomes negative because of the minor role of the spin–orbit scattering. For Au-films the spin–orbit scattering is so strong that it completely dominates the magneto-resistance.

The natural question is, why does weak localization change to weak anti-localization in the presence of spin–orbit scattering?

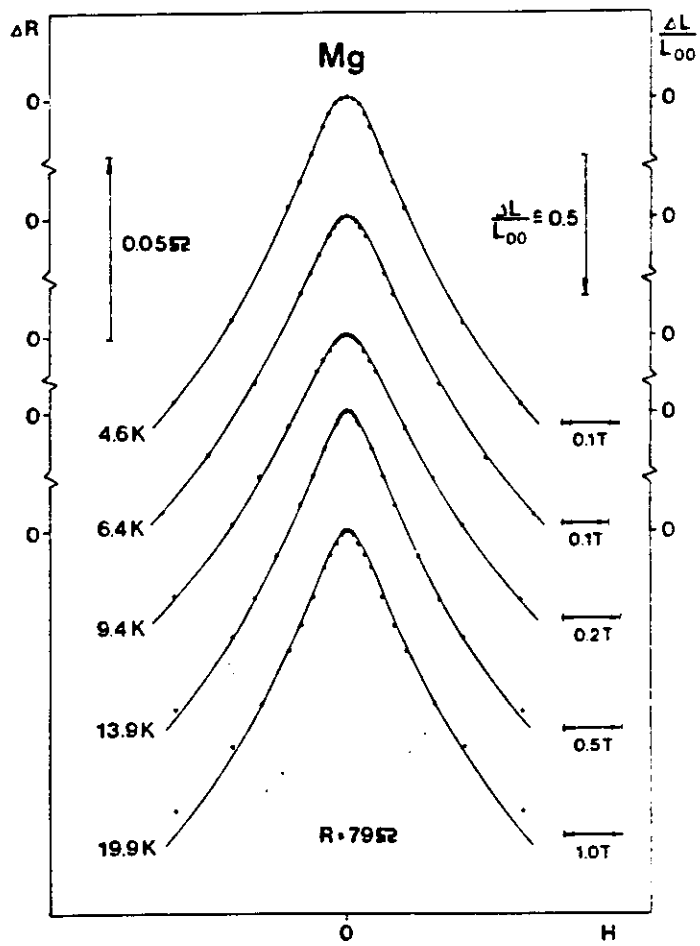

Fig. 2.11. The magneto-resistance of a thin Mg-film for different temperatures as a function of the applied field. The units of the field are given on the right of the curves. The points represent the experimental results. The full curves are calculated with the theory. The small spin–orbit scattering is taken into account.

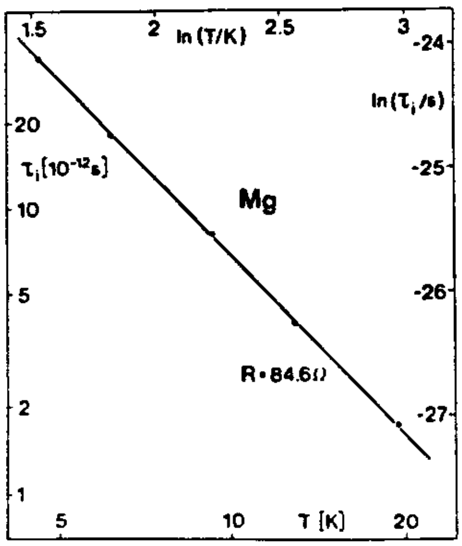

Fig. 2.12. The inelastic lifetime τ_i of a Mg-film as a function of temperature. It obeys a T^{-2}-law.

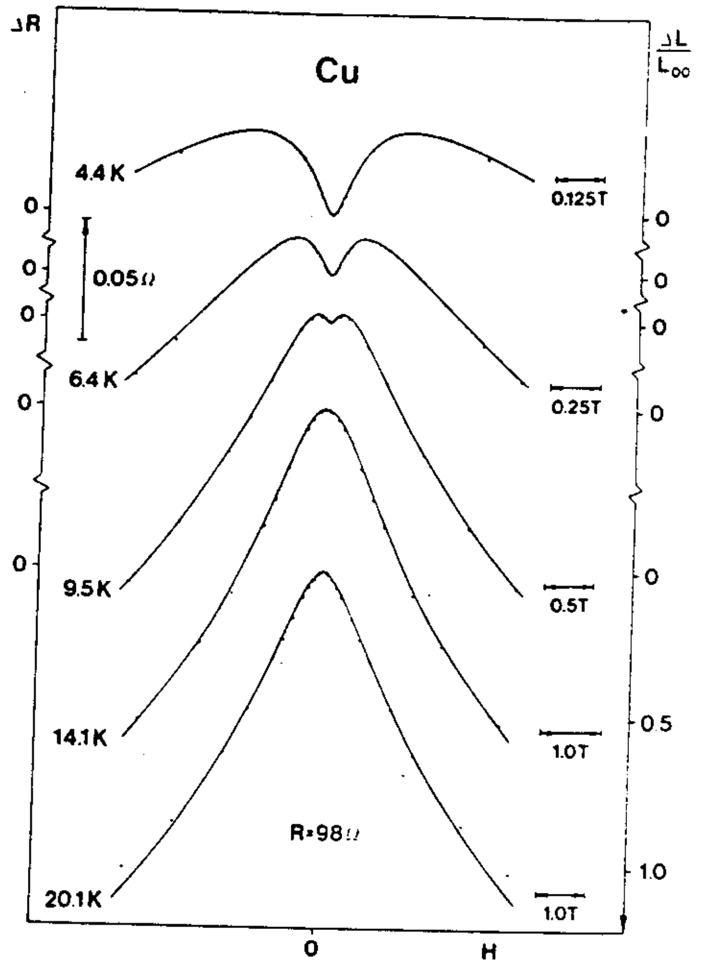

Fig. 2.13. The magneto-resistance of a Cu-film for different temperatures. The Cu possesses a natural spin–orbit scattering and therefore the pure metal shows the destructive interference of rotated spins. Again the points are experimentally measured whereas the full curves are calculated with the theory, adjusting the inelastic lifetime and the spin–orbit scattering time (expressed by the corresponding fields H_i and H_{so}).

2.4. Interference of rotated spins

It is a consequence of quantum theory and proved by a rather sophisticated neutron experiment that spin 1/2 particles have to be rotated by 4π to transfer the spin function into itself. A rotation by 2π reverses the sign of the spin state. Weak anti-localization gives another experimental proof of this fact. In the presence of spin–orbit scattering the matrix element for a transition from state k to k' has the form

$$V_{k-k}[1 - i\epsilon k \times k' * \sigma] \propto [1 - iK * \sigma]. \tag{2.10}$$

This matrix element describes a rotation of the electron spin by the angle K_i around the axis x_i ($i = 1, 2, 3$). During the whole scattering series (') the spin orientation diffuses into a final state σ' which can be obtained by a rotation T of the original spin state σ ($\sigma' = T\sigma$). It is straightforward to show that the finite spin state of the complementary scattering series (″) is $\sigma'' = T^{-1}\sigma$. Without the spin rotation the interference of the two partial waves is constructive (in the absence of an external field). In the presence of spin–orbit scattering the interference becomes destructive if the relative rotation of σ' and σ'' is 2π. It can be shown that for strong spin–orbit scattering the destructive part exceeds the constructive one [46]. This means that the back-scattering is reduced below the statistical one. This corresponds to an echo in the forward direction and a decrease of the resistance. The magneto-resistance curve in fig. 2.9b for 1% Au on top of Mg can be interpreted as follows. In a high magnetic field where $t_H < \tau_{so}$ the spin states of the complementary states are almost unchanged and one obtains the usual negative magneto-resistance. For $t_H > \tau_{so}$ (and $t_H < \tau_i$) the interference is destructive and shows the opposite sign. For $t_H \approx \tau_{so}$ it changes sign. The resistance maximum in a finite field corresponds to a relative rotation of σ' and σ'' by the angle π (in an average).

2.5. *Magnetic scattering*

Another interesting application of QUIAD is the determination of magnetic scattering by magnetic ions. The magnetic ion introduces an interaction with a conduction electron $J\,S*\sigma$, where S and σ are the ion and electron spins. The magnetic ions scatter the two complementary waves differently and destroy their coherence after the magnetic scattering time τ_s (see section 5).